

Influence of iron oxide green on smoke suppression properties and combustion behavior of intumescent flame retardant epoxy composites

Xilei Chen · Lei Liu · Jinlong Zhuo ·
Chuanmei Jiao

Received: 27 July 2014 / Accepted: 21 September 2014 / Published online: 10 October 2014
© Akadémiai Kiadó, Budapest, Hungary 2014

Abstract This article mainly studies smoke suppression properties and synergistic flame retardant effects of iron oxide green on intumescent flame retardant epoxy resins (IFREP) using ammonium polyphosphate and pentaerythritol as intumescent flame retardants. Then, the smoke suppression properties of iron oxide green ($\text{Fe}_2\text{O}_3 \cdot \text{H}_2\text{O}$) on intumescent flame retardant epoxy composites were evaluated using cone calorimeter test (CCT), smoke density test (SDT), scanning electron microscopy (SEM), thermogravimetric analysis-infrared spectrometry. Remarkably, CCT data reveal that a moderate amount of iron oxide green can apparently reduce heat release rate, total heat release, total smoke release, etc. On the other hand, the SDT results show that iron oxide green can catalyze the carbonization of IFREP at low temperature. Here, iron oxide green is considered to be an effective smoke suppression agent and a good synergism with IFR in flame retardant epoxy resins, which can greatly improve the structure of char residue realized by SEM results.

Keywords Smoke suppression · Iron oxide green · Flame retardant · Epoxy

Introduction

It has been reported that smoke produced in the fire is even the most important factor which directly puts people to death by poisoning and suffocation instead of burns [1, 2].

In many cases, the visibility impairing and narcotic irritating effect because of the evolution of smoke, toxic gases, and irritant compounds can prevent many fire victims from perceiving their possibilities of escape [3–7]. The inhalation of fire smoke, which contains not only carbon monoxide but also a complex mixture of gases, is the principal cause of morbidity and mortality in fire victims [8, 9]. Moreover, the high-temperature smoke containing a lot of heat can accelerate the spread of fire and cause thermal damage to people [10].

Epoxy resins are among the major commodity polymers in modern advanced composites because of their balance of excellent heat, solvent, moisture, and chemical resistance, good mechanical and electrical properties, and satisfactory adherence to many substrates [11–16]. However, its poor fire resistance is one of the main drawbacks in using epoxy thermosetting resins for the production of composites. Therefore, it is important to improve the flame retardancy of epoxy resins [17–23]. In a fire, halogen-containing flame retardants led to problems of smoke and possibly enhanced toxicity, and corrosion which has attracted considerable environmental attention [24–31]. Thus, a wide range of halogen-free flame retardants which are mostly phosphorus-containing flame retardants has been developed and used in epoxy resins. However, there is also a large amount of toxic smoke released from intumescent flame retardant epoxy composites during combustion. As a consequence, developing the retardants with good flame retardancy and smoke suppression is the key to further explore the epoxy resins applications.

Iron oxide green is commercially available as a pigment. It has been reported that iron oxide orange and iron oxide brown, in combination with polyphenylene oxide and preferably in further combination with borates such as zinc borate, provide a substantial degree of flame retardancy to

X. Chen · L. Liu · J. Zhuo · C. Jiao (✉)
College of Environment and Safety Engineering, Qingdao
University of Science and Technology,
Qingdao 266042, Shandong, People's Republic of China
e-mail: jiaochm@qust.edu.cn

polyamide 4,6 [32]. Iron oxide is one of the most effective char formers, and there is a linear correlation between smoke suppression and char formation [33]. Moreover, iron compounds acting as synergists and smoke suppressants in some thermoplastic polymer formulations have a catalytic action [34]. The nanocomposites based on iron oxide exhibit better thermal, flame retardant properties, smoke suppression, and lower degradation degree than those of pure polyvinyl chloride (PVC), poly(butylene terephthalate) (PBT), propylene (PP), recycled PET, and ethylene vinyl acetate copolymer/layered double hydroxides (EVA/LDH) nanocomposites [35–37]. To the best of our knowledge, no work has been reported the synergistic effects between iron oxide green and IFR on the achievement of smoke suppression and flame retardant properties in epoxy resins.

This paper mainly studies the synergistic smoke suppression properties and flame retardant effect between iron oxide green and IFR in flame retardant epoxy resins. Then, the effect was investigated by cone calorimeter test (CCT), smoke density test (SDT), thermogravimetric analysis-infrared spectrometry (TG-IR). In addition, to further explore how the structure of char determines smoke suppression properties, the residue chars of flame retardant epoxy composites left after CCT were examined by scanning electron microscopy (SEM) analysis.

Experimental

Materials

Epoxy resin (bisphenol A epoxy acrylate resin), used as film-forming material, was purchased from the Stanley Technology Co. Ltd., Shijiazhuang, China; Methyltetrahydrophthalic Anhydride (MTHPA; 98 % pure) curing agent was from Sitanlei Co. Ltd., Shijiazhuang, China; ammonium polyphosphate (APP) with particle size of 2,500 mesh was supplied by Keyan Institute of Chemical Engineering, Hefei, China; PER with particle size of 2,500 mesh was purchased from new thin Metal and Chemical Co., Ltd., Guangzhou, China; intumescent flame retardant was obtained with the mass ratio of APP and PER is 3:1; iron oxide green with particle size of 8.75 μm was purchased from the Zhicheng Trade Co., Ltd., Qingdao, China.

Preparation of samples

EP was mixed with iron oxide green at room temperature using a high-speed disperser for 1.0 h to yield the blend. Then, IFR was added into the blend, and stirred for 1.0 h. At last, MTHPA was added and stirred for 1.0 h. And the

Table 1 The formulations of flame retardant epoxy composites

Sample code	Epoxy/mass%	MTHPA/mass%	IFR/mass%	Iron oxide green/mass%
EP-0	55.6	44.4	–	–
EP-1	39.0	31.0	30.0	–
EP-2	39.0	31.0	29.5	0.5
EP-3	39.0	31.0	29.0	1.0
EP-4	39.0	31.0	28.0	2.0
EP-5	39.0	31.0	27.0	3.0

listing order is given in Table 1. The mixture was cured under 80 °C for 8.0 h, and 150 °C for 3.0 h to obtain flame retardant epoxy composites.

Measurements

Cone calorimeter

The cone calorimeter (Stanton Redcroft, UK) tests were performed according to ISO 5660 standard procedures. Each specimen of dimensions 100 × 100 × 3 mm³ was wrapped in aluminum foil and exposed horizontally to an external heat flux of 50 kW m⁻².

Smoke density test (SDT)

A SDT machine JQMY-2 (Jianqiao Co, China) was used to measure the smoke characteristics according to ISO 5659-2 (2006). Each specimen of dimensions 75 × 75 × 2.5 mm³ was wrapped in aluminum foil and exposed horizontally to an external heat flux of 25 kW m⁻² with the application of a pilot flame.

Scanning electron microscope (SEM)

Scanning electron microscope (SEM, JSM-6700F) was used to examine the structures of char residues after CCT. The samples were coated with a thin layer of gold by sputtering before the SEM imaging. An accelerating voltage of 5 kV was applied.

Thermogravimetric analysis/infrared spectrometry (TG-IR)

TG-IR of the sample was performed using a DT-50 (Setaram, France) instrument that was interfaced to a FTIR (SENSOR27, Bruker Co. Germany) spectrometer. About 10.0 mg of sample was put in an alumina crucible and heated from ambient temperature to 750 °C. The heating rates were set as 20 K min⁻¹ (nitrogen atmosphere, flow rate of 20 mL min⁻¹).

Results and discussion

Cone calorimeter test

Heat release rate

Figure 1 shows the heat release rate (HRR) curves of all EP samples in the CCT. CCT can be used as an effective approach to compare and evaluate the combustion behavior of polymer materials. HRR, especially peak heat release rate (PHRR) has been found to be a very important parameter as it expresses the intensity of a fire, which in turn determines other parameters. It can be seen that EP-0 burns very fast after ignition; the ignition time is 50 s, and the PHRR of 922 kW m^{-2} is obtained at 189 s. EP-0 has a single peak, which can easily be explained by the sample gradually burning. When IFR is added to the EP system, each sample has multi-peak phenomena. The appearance of the first peak indicates the start of burning, then the HRR drops because of the formation of an insulating char layer. The second peak arises because the temperature increases on the unexposed surface with the partial destruction of the charred material [38]. For EP-1 with only IFR, the ignition time is 75 s which is longer than that of EP-0; the first PHRR value of EP-1 is 130 kW m^{-2} , and the second PHRR value is 257 kW m^{-2} which is much lower than that of EP-0. The reason is that the APP release ammonia at the beginning of heating, and polyphosphoric acid produced by the elimination of ammonia from APP can attack hydroxyl bonds of PER with formation of phosphoric ester. The phosphoric ester can thermally decompose at higher temperatures, leading to formation of three-dimensional network structures. Furthermore, the C–H bonds for EP are dehydrogenated and oxidized with formation of C–O–OH groups on the backbone. Then the crosslinking occurs between EP and IFR, and a complicated network could be formed which could act as a barrier to prevent heat to underlying materials and flammable gases into flame zone [39, 40]. In the case of the samples with both IFR and iron oxide green, the first PHRR values are greatly reduced to 102, 91, 114, and 180 kW m^{-2} , respectively. And the second PHRR values are 172, 196, 186, and 225 kW m^{-2} , respectively. It can be approved that the presence of iron oxide green could promote the release of ammonia from APP, and form Fe^{n+} because of multiple valency of Fe. At the same time APP could react with Fe^{n+} which takes as bridges, the formation would increase the molecular weight and led to a stabilization of the APP, which could increase the viscosity of the melt during pyrolysis and combustion [41]. It should be pointed out that the first PHRR value of EP-5 is higher than that of EP-1. It can be explained by that when increasing the mass of the iron, the negative effect could exceed the positive effect on the fire properties, due

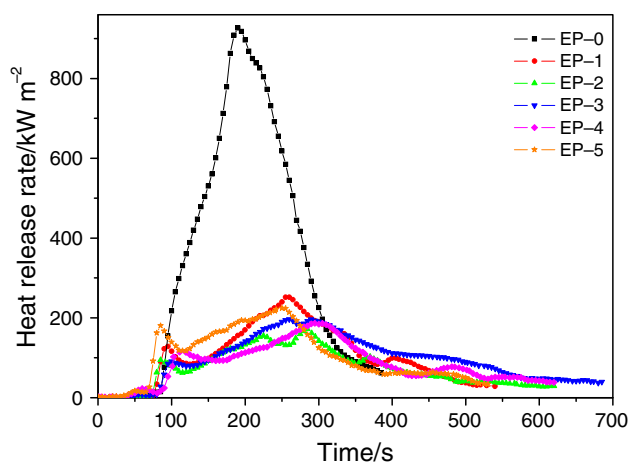


Fig. 1 Heat release rates of flame retardant epoxy samples

to reducing the content of IFR [41]. Moreover, the HRR curves of the samples with both IFR and iron oxide green are very flat, and the addition of iron oxide green strongly prolongs the combustion time compared with EP-1. The ignition times of the samples from EP-2 to EP-5 are 28, 40, 52, 43 s, respectively. It can be obviously seen that the ignition times of the samples with both IFR and iron oxide green are much shorter than that of EP-1 with only IFR. The reason is due to the fact that the samples with different additives show different thermal response behaviors in the CCT. Some samples which expand before ignition in the CCT could lead to the distance between the surface of the sample and cone small. Meanwhile, the radiation heat flux will increase, which can accelerate EP decomposing, resulting short ignition time. Furthermore, the expansion process is not uniform [42]. According to the phenomenon above, it is deduced that the addition of IFR and iron oxide green can remarkably enhance the flame retardancy of flame retardant composites.

Mass

Figure 2 shows the percentage of residual mass of flame retardant epoxy composites in the CCT. It can be seen from Fig. 2 that mass loss of EP-0 is very large, just 2 mass% remained at 390 s. However, EP-1 with only IFR reaches the final constant value (45 mass%) at approximately 530 s. It can be explained by the addition of IFR forming a protective rigid layer during the combustion process, which acts as a barrier for heat and mass transfer. However, this layer is not compact enough and breaks quickly resulting large mass loss. The char residue mass of the samples containing IFR and iron oxide green is 56, 48, 58, and 53 mass%, which are much higher than that of EP-1. And EP-

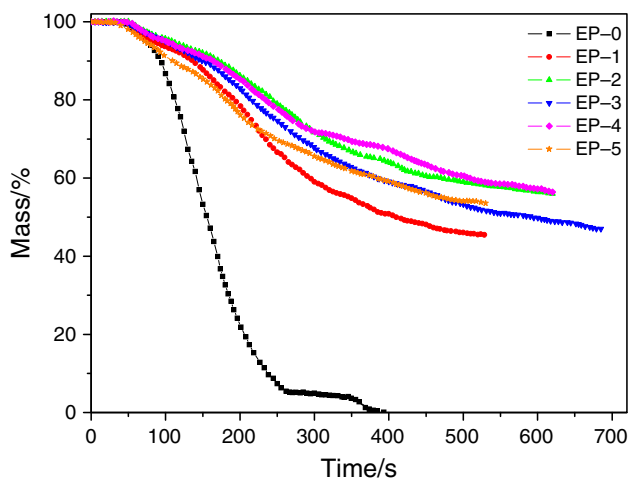


Fig. 2 Mass loss curves of flame retardant epoxy samples

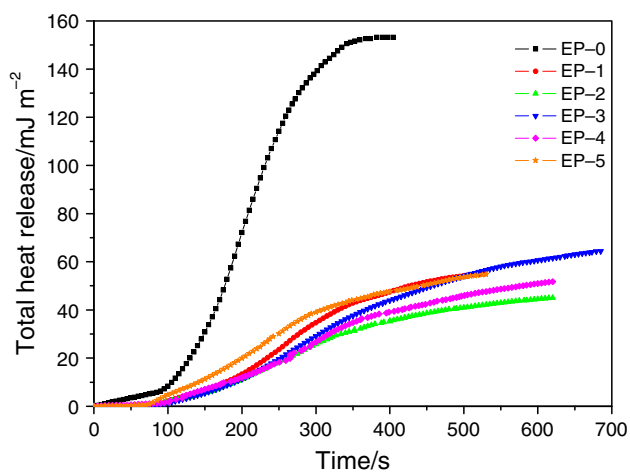


Fig. 3 Total heat release of flame retardant epoxy samples

4 shows the highest char residue among all flame retardant samples. In addition, the samples with IFR and iron oxide green begin degradation earlier than EP-0 and reach constant mass after approximately 450 s, but the mass loss rate is much lower than that of EP-0 and EP-1. It knows that an early decomposition of the intumescent flame retardant system is necessary to increase the fire-proofing properties of the material [43, 44]. This result also means that there is catalyzing carbonization effect by iron oxide green in the intumescent flame retardant epoxy composites, and a compact char residue forms on the surface of the sample in the combustion process.

Total heat release

Figure 3 presents the total heat release (THR) curves for all samples. THR depends on carbonaceous charring, fuel dilution—including the replacement of polymer in the condensed phase, and flame inhibition—mainly reducing

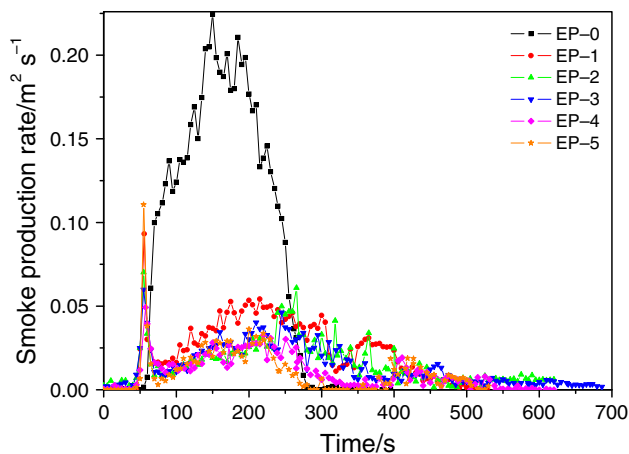


Fig. 4 Smoke produce rates of flame retardant epoxy samples

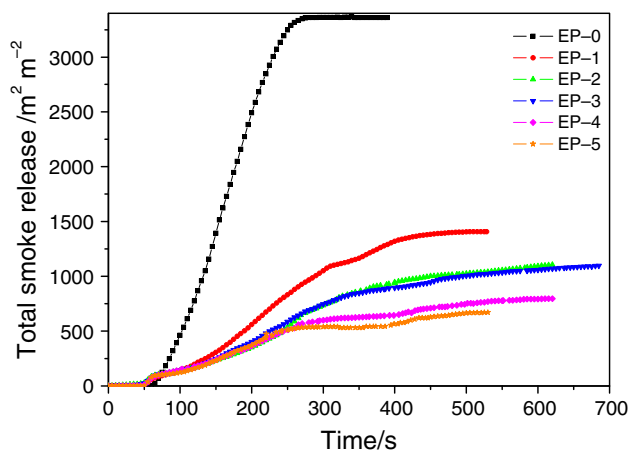


Fig. 5 Total smoke release of flame retardant epoxy samples

combustion efficiency in the flame [34]. The slope of THR curve can be assumed as representative of fire spread [45]. From Fig. 3, it can be seen that the THR value (152 mJ m^{-2}) of EP-0 is the highest among all samples. Compared with EP-0, the gradient of THR curve from EP-1 with only IFR is greatly reduced, indicating the flame spread speed slows down. In the case of the samples containing both IFR and iron oxide green, the flame spread speed further decreases. The reason is that the iron oxide green could serve to generate beneficial intumescent char layers in the intumescent flame retardant epoxy resins (IFREP) composites, restricting flames spread.

Smoke production rate

Smoke performance of flame retardant material is regarded as a significant parameter in fire safety fields. The smoke production rate (SPR) curves of flame retardant epoxy composites are illustrated in Fig. 4. The peak SPR values of EP-0 and EP-1 are 0.224 and $0.093 \text{ m}^2 \text{ s}^{-1}$, respectively.

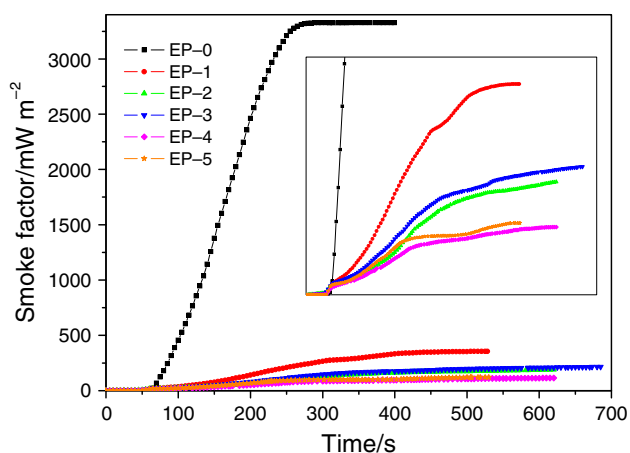


Fig. 6 Smoke factors of flame retardant epoxy samples

It obviously takes on a significant decrease with the addition of the IFR. However, the time to peak SPR of EP-1 is much shorter than that of EP-0. That is because at the initial stage of heating, the surface temperature raises quickly, resulting in the rapid decomposition of IFR and formation of smoke particles on the surface of EP-1. The peak SPR values of samples containing both IFR and iron oxide green are 0.072, 0.061, 0.048, and 0.112 $\text{m}^2 \text{s}^{-1}$, respectively. It can be seen that the curves and the values of the samples with IFR and iron oxide green are far lower than those of EP-0 and EP-1, which has the homologous phenomenon with the HRR in the CCT. Also, it should be pointed out that the time to the peak SPR value of all samples are 151, 55, 54, 55, 55, and 56 s, respectively. Smoke suppression by iron oxide green and IFR can be explained as follows: moderate content of iron oxide green and IFR can promote charring and enhance the quality of char, which can protect the inner matrix and reduce the amount of combustible gas and smoke-forming materials in the gas phase during combustion [33]. In the case of EP-4 with 28.0 mass% IFR and 2.0 mass% iron oxide green, iron oxide green can efficiently catalyze IFREP to form thick char residue at the beginning of the CCT.

Total smoke release

The total smoke release (TSR) values of flame retardant epoxy composites are illustrated in Fig. 5. As is portrayed in Fig. 5, the distinction between EP-0 and the flame retarded samples is apparent after 70 s. The TSR values of all samples are 3,364, 1,407, 1,105, 1,097, 796, and 670 $\text{m}^2 \text{m}^{-2}$, respectively. It is obvious that the TSR values significantly decrease with the addition of iron oxide green. The reason for the TSR greatly decreasing with the addition of iron oxide green is the smoke suppression properties of iron oxide green. The smoke suppression mechanism by iron oxide green in burning IFREP is a combination of several

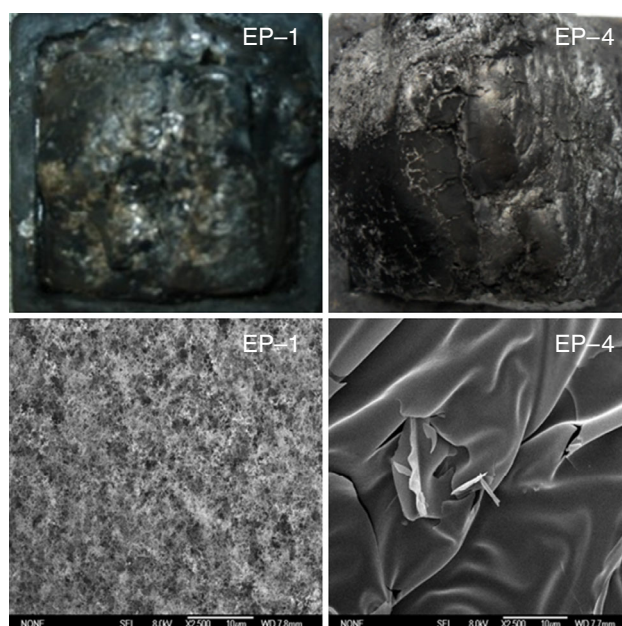


Fig. 7 Digital photographs and SEM of char residue of flame retardant epoxy samples after CCT

interrelated effects. First, the reaction between iron oxide green and APP can increase the viscosity of the melt and the stability of the char layer during the process of pyrolysis and combustion, and thus prevent combustible gases from diffusing into air. Second, some studies have shown that Fe^{n+} ions behave as an ideal radical scavenger which can restrain the attack of the free radicals. So it is also effective in chemically removing certain volatile fuels which are responsible for promoting the burning of the specimens and the formation of smoke particulates [46, 47].

Smoke factor

Figure 6 presents the smoke factor (SF) as a function of time for all samples. SF is the product of PHRR and TSR [48]. The SF value of EP-0 is up to 3,322 mW m^{-2} . And the SF value of EP-1 is only 351 mW m^{-2} , which is much lower than that of EP-0. It is very obvious that the addition of IFR significantly reduces the SF values of intumescent flame retardant epoxy composites. Furthermore, the samples containing both IFR and iron oxide green show further decrease in SF values compared with EP-1. The SF values of the samples with both IFR and iron oxide green are 195, 215, 113, and 125 mW m^{-2} , respectively. That indicates the same conclusion with the above results of SPR and TSR.

Sem

Figure 7 is the photographs and SEM of char residues for EP-1 and EP-4 after CCT. The char layer formation

on the surface of cured epoxy samples could prevent heat and oxygen from transferring into the underlying materials, and flammable volatiles into flame zone. From Fig. 7, it is clear that the char residue of EP-1 is the light and loose responding. As well, it can be observed that there are some holes existed in the surface. It is due to the instantaneous release of a large amount of NH_3 by APP/PER, which was likely to have formed large pores in the char [49]. In contrast, the char residue of EP-4 shows a compact appearance and smooth surface. Holes and crevices are nearly not existed in the char residue of EP-4. It can be concluded that the addition of IFR forms a protective rigid layer during the combustion; however, this layer breaks quickly. The adding of iron oxide green modifies the rigid layer, and during the entire combustion process, the material grows thicker; after complete combustion, the compact layer still remains as a whole.

Smoke density test (SDT)

Figure 8 shows the luminous flux curves of flame retardant epoxy composites with flame in the SDT. In the case of EP-0, the luminous flux slightly decreases and gets the lowest luminous flux value (88.7 %) at 1,200 s. When IFR is added into epoxy resins, the luminous flux mainly decreases from 725 s, and attains the lowest value (56.4 %) at 1,200 s in the SDT. That is due to the low decomposition temperature of APP. In the case of the samples containing both IFR and iron oxide green, the luminous flux can further decrease compared with EP-1 containing only IFR. Here, the addition of iron oxide green could promote the release of ammonia from APP and form Fe^{n+} which could react with APP.

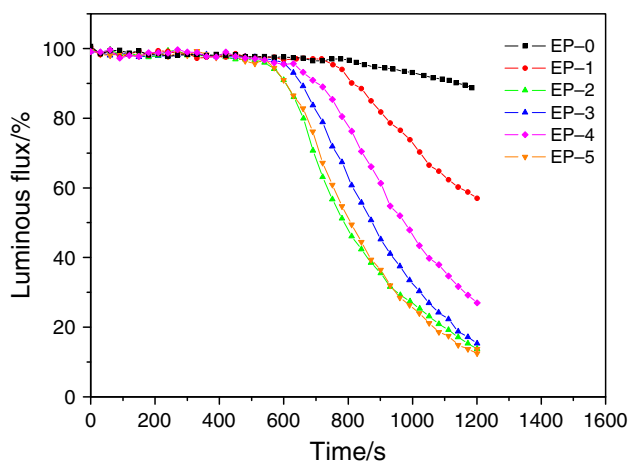


Fig. 8 Luminous flux of flame retardant epoxy samples

FTIR characterization of EP-0/EP-1/EP-4 composites

Figure 9 presents 3D TG-FTIR spectra of pyrolysis products of the flame retardant epoxy samples during thermal degradation. It can be seen that the evolved gas products for the three samples exhibit characteristic bands of 3,230–3,550, 2,800–3,150, 2,250–2,400, 1,700–1,850, 1,250–1,500, and 950–1,150 cm^{-1} . The spectra fit well with the reported FTIR features of gas products such as H_2O (3,230–3,550 cm^{-1}), CO_2 (2,300–2,400 cm^{-1}), CO

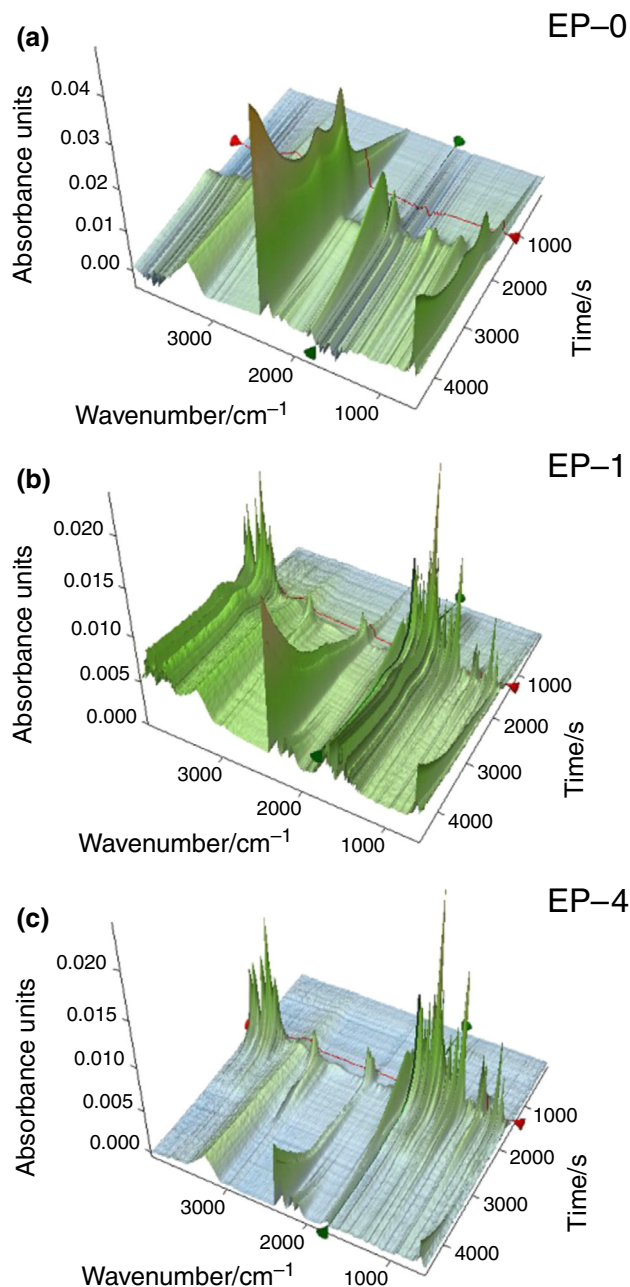


Fig. 9 The 3D TG-FTIR spectra of pyrolysis products of the composites during the thermal degradation: a EP-0, b EP-1, and c EP-4

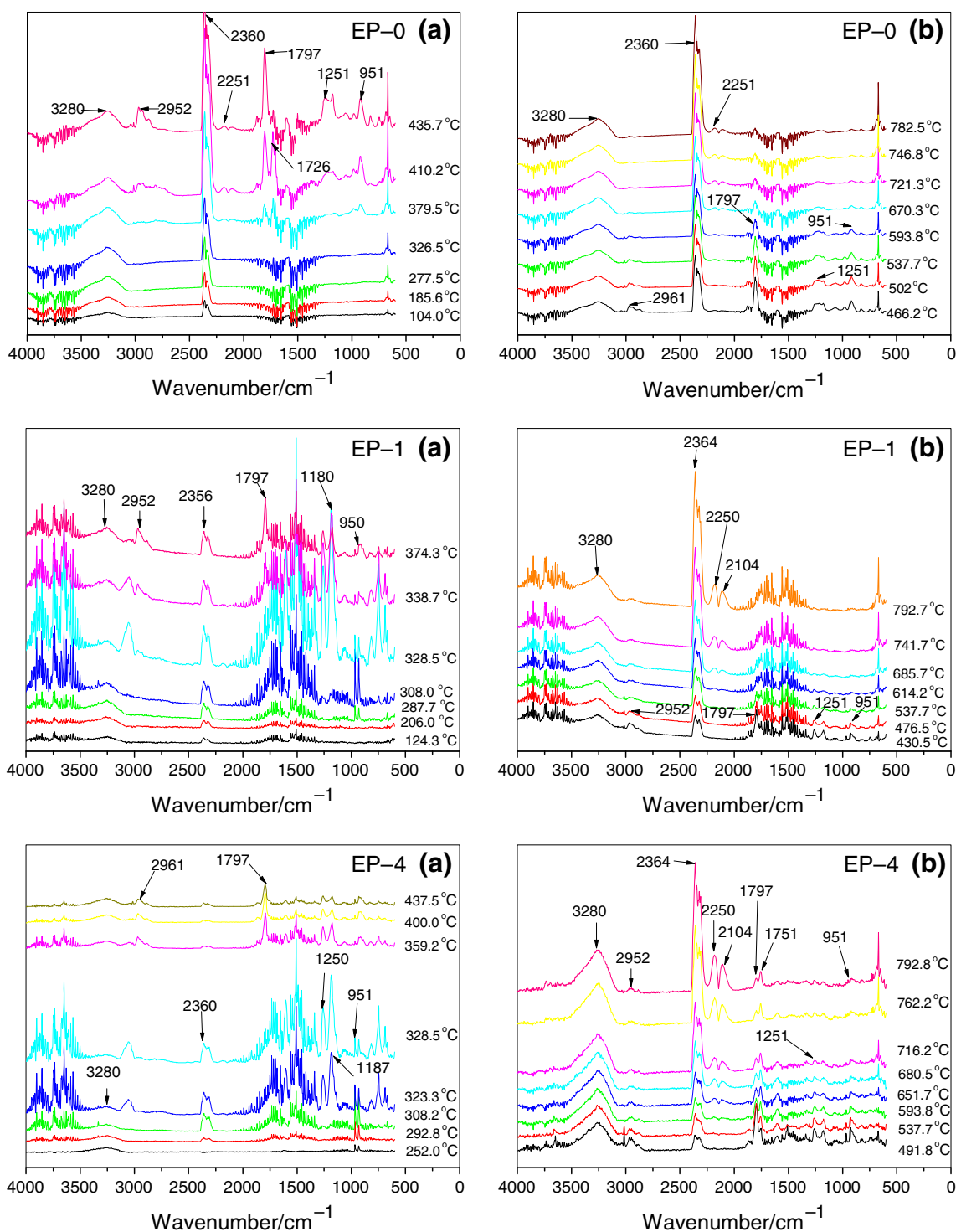


Fig. 10 FTIR spectra of pyrolysis products of the composites at different temperatures: EP-0 (a, b), EP-1 (a, b), and EP-4 (a, b)

(2,250–2,300 cm^{-1}), carboxylic acid (1,700–1,850 cm^{-1}), and aliphatic hydrocarbons (2,800–3,150, 1,250–1,500, and 950–1,150 cm^{-1}). As a matter of fact, the main decomposition products of the composites are H_2O , CO_2 , CO, carboxylic acid, and aliphatic hydrocarbons.

It is obvious that the decomposition processes of the three samples are significantly different. EP-0 decomposes drastically when heated, producing lots of CO_2 , CO, carboxylic acid, and aliphatic hydrocarbons. Moreover, the decomposition of EP-1 with only IFR is slowed

down. Furthermore, the decomposition of EP-4 is slowed down further when iron oxide green is added into the composites.

Figure 10 shows the characteristic spectra obtained from 30 to 900 °C. As in the case of EP-0, there is almost no infrared signal below 104 °C (124.3 °C for EP-1, 292.8 °C for EP-4), indicating that the composites do not decompose under this temperature. The release of H₂O, CO₂, and CO could be detected with the temperature increasing. When the temperature increases to 435.7 °C (374.3 °C for EP-1, 491.8 °C for EP-4), a maximum signal intensity appears at 1,700–1,850 cm⁻¹ due to the fact that carboxylic acid is observed. This can be attributed to the existence of methyltetrahydrophthalic anhydride and APP. And a maximum signal at 2,800–3,150 cm⁻¹ attributed to aliphatic hydrocarbons is observed at 435.7 °C (374.3 °C for EP-1, 491.8 °C for EP-4). Moreover, CO₂ and CO release gradually increase with increasing temperature. These phenomena can be clarified that during the thermal degradation of IFREP, that the formations of carbonic anhydride structures further decompose can lead to the elimination of volatilized CO and CO₂ by the formations of alkane, and aromatic compounds [50]. As it was expected, the signal intensity of the pyrolysis products declined gradually, implying that the decomposition rate of the mixture is slowed down.

Conclusions

As to all the results of intumescent flame retardant epoxy resin containing iron oxide green (IFREP/iron oxide green) tested by CCT, SDT, SEM, and FTIR, we can draw the following conclusions. First, iron oxide green can help to change the structure of char residue layer that restrain the heat release and smoke generation. Second, iron oxide green represents dramatically excellent smoke suppression properties in flame retardant epoxy composites based on IFR. Third, the synergistic flame retardant effect and smoke suppression between iron oxide green and IFR are very apparent. In summary, the synergistic smoke suppression and flame retardant properties between iron oxide green and IFR in epoxy composites are excellent. Combining iron oxide green and IFR as a system has the wide application prospect in smoke suppression fields.

Acknowledgements The authors gratefully acknowledge the National Natural Science Foundation of China (No.51106078; 51206084) and the Out-standing Young Scientist Research Award Fund from Shandong Province (BS2011CL018).

References

- Dong Y, Gui Z, Hu Y. The influence of titanate nanotube on the improved thermal properties and the smoke suppression in poly(methyl methacrylate). *J Hazard Mater*. 2012;209:34–9.
- Yan YW, Chen L, Jian RK. Intumescence: an effect way to flame retardance and smoke suppression for polystyrene. *Polym Degrad Stab*. 2012;97(8):1423–31.
- Purser DA. Toxic product yields and hazard assessment for fully enclosed design fires. *Polym Int*. 2000;49(10):1232–55.
- Cassuto J, Tamow P. The discotheque fire in Gothenburg 1998: a tragedy among teenagers. *Burns*. 2003;29(5):405–16.
- Beyer G. Flame retardant properties of EVA-nanocomposites and improvements by combination of nanofillers with aluminium trihydrate. *Fire Mater*. 2001;25(5):193–7.
- Martinka J, Kačíková D, Hroncová E, Ladomerský J. Experimental determination of the effect of temperature and oxygen concentration on the production of birch wood main fire emissions. *J Therm Anal Calorim*. 2012;110(1):193–8.
- Ye L, Zhang Y, Wang S, Gao G, Liu J, Zhou Y, Liu H. Synergistic effects and mechanism of ZnCl₂ on intumescent flame-retardant polypropylene. *J Therm Anal Calorim*. 2014;115(2):1065–71.
- Hu LH, Fong NK, Yang LZ. Modeling fire-induced smoke spread and carbon monoxide transportation in a long channel: fire dynamics simulator comparisons with measured data. *J Hazard Mater*. 2007;140(1):293–8.
- Omaye ST. Metabolic modulation of carbon monoxide toxicity. *Toxicology*. 2002;180(2):139–50.
- Zhou R, Zhang W, Zhao D. Computational simulation of smoke temperature diffusion in high-rise buildings fires. *Res J Appl Sci Eng Technol*. 2013;5(6):2078–83.
- Kinjo N, Ogata M, Nishi K, Kaneda A. Epoxy molding compounds as encapsulation materials for microelectronic devices. *Adv Polym Sci*. 1989;1–48.
- Chen H, Jacobs O, Wu W. Effect of dispersion method on tribological properties of carbon nanotube reinforced epoxy resin composites. *Polym Test*. 2007;26(3):351–60.
- Guo Y, Bao C, Song L. In situ polymerization of graphene, graphite oxide, and functionalized graphite oxide into epoxy resin and comparison study of on-the-flame behavior. *Ind Eng Chem Res*. 2011;50(13):7772–83.
- Wu K, Song L, Hu Y. Synthesis and characterization of a functional polyhedral oligomeric silsesquioxane and its flame retardancy in epoxy resin. *Prog Org Coat*. 2009;65(4):490–7.
- Guo Q, Huang Y, Zhang YY, Zhu LR, Zhang BL. Curing behavior of epoxy resins with a series of novel curing agents containing 4,4'-biphenyl and varying methylene units. *J Therm Anal Calorim*. 2010;102(3):915–22.
- Jiao CM, Zhuo JL, Chen XL, Li SX, Wang H. Flame retardant epoxy resin based on bisphenol A epoxy resin modified by phosphoric acid. *J Therm Anal Calorim*. 2013;114(1):253–9.
- Wang X, Hu Y, Song L. Thermal degradation mechanism of flame retarded epoxy resins with a DOPO-substituted organophosphorus oligomer by TG-FTIR and DP-MS. *J Anal Appl Pyrolysis*. 2011;92(1):164–70.
- Bao C, Guo Y, Song L. In situ preparation of functionalized graphene oxide/epoxy nanocomposites with effective reinforcements. *J Mater Chem*. 2011;21(35):13290–8.
- Azeez AA, Rhee KY, Park SJ. Epoxy clay nanocomposites—processing, properties and applications: a review. *Compos Part B-Eng*. 2013;45(1):308–20.
- Wan J, Li C, Bu ZY. A comparative study of epoxy resin cured with a linear diamine and a branched polyamine. *Chem Eng J*. 2012;188:160–72.

21. Cheng XE, Shi W. Synthesis and thermal properties of silicon-containing epoxy resin used for UV-curable flame-retardant coatings. *J Therm Anal Calorim.* 2011;103(1):303–10.
22. Gao M, Wu W, Yan Y. Thermal degradation and flame retardancy of epoxy resins containing intumescent flame retardant. *J Therm Anal Calorim.* 2009;95(2):605–8.
23. Agrawal S, Narula AK. Curing and thermal behaviour of a flame retardant cycloaliphatic epoxy resin based on phosphorus containing poly(amide-imide)s. *J Therm Anal Calorim.* 2014;115(2):1693–703.
24. Mauerer O. New reactive, halogen-free flame retardant system for epoxy resins. *Polym Degrad Stab.* 2005;88(1):70–3.
25. Lin HT, Lin CH, Hu YM. An approach to develop high- T_g epoxy resins for halogen-free copper clad laminates. *Polymer.* 2009;50(24):5685–92.
26. Perez RM, Sandler JKW, Altstädt V. Effective halogen-free flame retardants for carbon fibre-reinforced epoxy composites. *J Mater Sci.* 2006;41(15):4981–4.
27. Perez RM, Sandler JKW, Altstädt V. Effective halogen-free flame retardancy for a monocomponent polyfunctional epoxy using an oligomeric organophosphorus compound. *J Mater Sci.* 2006;41(24):8347–51.
28. Levchik S, Piotrowski A, Weil E. New developments in flame retardancy of epoxy resins. *Polym Degrad Stab.* 2005;88(1):57–62.
29. Darnerud PO. Toxic effects of brominated flame retardants in man and in wildlife. *Environ Int.* 2003;29:841–53.
30. Lu SY, Hamerton I. Recent developments in the chemistry of halogen-free flame retardant polymers. *Prog Polym Sci.* 2002;27:1661–712.
31. Xie R, Qu B. Synergistic effects of expandable graphite with some halogen-free flame retardants in polyolefin blends. *Polym Degrad Stab.* 2001;71:375–80.
32. Weil ED, Patel NG. Iron compounds in non-halogen flame-retardant polyamide systems. *Polym Degrad Stab.* 2003;82:291–6.
33. Levchik SV, Weil ED. Review overview of the recent literature on flame retardancy and smoke suppression in PVC. *Polym Adv Technol.* 2005;16:707–16.
34. Gallo E, Schartel B, Braunb U, Russoa P, Acierno D. Fire retardant synergisms between nanometric Fe_2O_3 and aluminum phosphinate in poly(butylene terephthalate). *Polym Adv Technol.* 2011;22:2382–91.
35. Zhang B, Yan XY, Shibata K. Thermogravimetric-mass spectrometric analysis of the reactions between oxide (ZnO , Iron oxide green or $ZnFe_2O_4$) and polyvinyl chloride under inert atmosphere. *Mater Trans.* 2000;41:1342–50.
36. Laoutid F, Ferry L, Lopez-Cuesta JM, Crespy A. Flame-retardant action of red phosphorus/magnesium oxide and red phosphorus/iron oxide compositions in recycled PET. *Fire Mater.* 2006;30:343–58.
37. Kashiwagi T, Grulke E, Hilding J, Harris R, Awad W, Douglas J. Thermal degradation and flammability properties of poly(propylene)/carbon nanotube composites. *Macromol Rapid Commun.* 2002;23:761–5.
38. Duquesne S, Samyn F, Bourbigot S. Influence of talc on the fire retardant properties of highly filled intumescent polypropylene composites. *Polym Adv Technol.* 2008;19:620–7.
39. Kandola BK, Horrocks AR. Complex char formation in flame-retarded fibre-intumescent combinations—II. Thermal analytical studies. *Polym Degrad Stab.* 1996;54(2):289–303.
40. Tang Y, Hu Y, Song L, Zong RW, Gui Z, Fan WC. Preparation and combustion properties polypropylene-polyamide-6 of flame retarded alloys. *Polym Degrad Stab.* 2006;91(2):234–41.
41. Zhang P, Hu Y, Song L, Lu HD, Wang J, Liu QQ. Synergistic effect of iron and intumescent flame retardant on shape-stabilized phase change material. *Thermochim Acta.* 2009;487:74–9.
42. Chen XL, Jiang YF, Jiao CM. Smoke suppression properties of ferrite yellow on flame retardant thermoplastic polyurethane based on ammonium polyphosphate. *J Hazard Mater.* 2014;266:114–21.
43. Cai YB, Li Q, Wei QF, Wu YB, Song L, Hu Y. Structures, thermal stability, and crystalline properties of polyamide 6/organic-modified Fe-montmorillonite composite nanofibers by electrospinning. *J Mater Sci.* 2008;43(18):6132–8.
44. Ullah S, Ahmad F, Megat-Yusoff PSM. Effect of boric acid with kaolin clay on intumescent fire retardant coating. *J Appl Sci.* 2011;11(21):3645–9.
45. Chiang CL, Ma CCM. Synthesis, characterization and thermal properties of novel epoxy containing silicon and phosphorus nanocomposites by sol-gel method. *Eur Polym J.* 2002;38:2219–24.
46. Marinović-Cincović M, Popović MČ, Novaković MM. The influence of β -FeOOH nanorods on the thermal stability of poly(methyl methacrylate). *Polym Degrad Stab.* 2007;92(1):70–4.
47. Carty P, White S, Price D. Smoke-suppression in plasticised chlorinated poly(vinyl chloride) (CPVC). *Polym Degrad Stab.* 1999;63(3):465–8.
48. Ricciardi MR, Antonucci V, Zarrelli M, Giordano M. Fire behavior and smoke emission of phosphate-based inorganic fire-retarded polyester resin. *Fire Mater.* 2012;36:203–15.
49. Wu N, Yang RJ. Effects of metal oxides on intumescent flame-retardant polypropylene. *Polym Adv Technol.* 2011;22:495–501.
50. Chen XL, Jiao CM. Thermal degradation characteristics of a novel flame retardant coating using TG-IR technique. *Polym Degrad Stab.* 2008;93:2222–5.